Design of the thermal neutron detection system for CJPL-II *

Zhao-Ming Zeng(曾昭明)[1,2;1)] Hui Gong(宫辉)[1,2;2)] Jian-Min Li(李荐民)[1,2;3)]
Qian Yue(岳骞)[1,2;4)] Zhi Zeng(曾志)[1,2;5)] Jian-Ping Cheng(程建平)[1,2;6)]

[1] Department of Engineering Physics, Tsinghua University, Beijing 100084, China
[2] Key Laboratory of Particle and Radiation Imaging (Ministry of Education), Tsinghua University, Beijing 100084, China

Abstract: A low background thermal neutron flux detection system has been designed to measure the ambient thermal neutron flux of the second phase of the China Jinping Underground Laboratory (CJPL-II), right after completion of the rock bolting work. A ^{3}He proportional counter tube combined with an identical ^{4}He proportional counter tube was employed as the thermal neutron detector, which has been optimised in energy resolution, wall effect and radioactivity of construction materials for low background performance. The readout electronics were specially designed for long-term stable operation and easy maintenance in an underground laboratory under construction. The system was installed in Lab Hall No. 3 of CJPL-II and accumulated data for about 80 days. The ambient thermal neutron flux was determined under the assumption that the neutron field is fully thermalized, uniform and isotropic at the measurement position.

Keywords: thermal neutron background, CJPL-II, underground laboratory, ^{3}He proportional tube

PACS: 29.40.Cs **DOI:** 10.1088/1674-1137/41/5/056002

1 Introduction

Rare-event experiments are mainly carried out in deep underground laboratories, which benefit from cosmic ray shielding. China Jinping Underground Laboratory (CJPL), with an average rock overburden of 2.4 kilometres, is the deepest underground laboratory in the world [1]. There are two experiments, CDEX [2] and PandaX [3], currently running at CJPL, both of which have published competitive physics results. The laboratory is currently undergoing a large scale expansion. This second phase of CJPL will increase laboratory space to approximately 96000 m^3, whereas the existing CJPL-I has a volume of $\sim$ 4000 m^3 [4]. There are many experiments planned for CJPL-II, including tonne-scale versions of the dark matter search experiments, precision measurements of solar neutrinos, and measurement of the rates of astrophysically important stellar nuclear reactions. The environmental background should be determined to provide environmental parameters for rare-event experiments to be carried out at CJPL-II.

Thermal neutrons are not only an annoying background component due to nuclide activation, but also reflect the level of fast neutrons. Thermal neutron flux is a significant environmental parameter for an underground laboratory. The main neutron source of the underground laboratory is from the natural radioactivity of the rock via spontaneous fission and (α, n) reactions [5, 6]. In general, the ambient thermal neutron flux of underground laboratories is at the level of 10^{-6} cm^{-2}·s^{-1} [7, 8], three orders of magnitude lower than at ground level. The detection system should have high sensitivity and low background counting rate in the region of interest (ROI) to get precise results in an acceptable measuring time.

A low background thermal neutron flux detection system was designed, which was then installed in Lab Hall No. 3 of CJPL-II after the rock bolting work, and accumulated data for about 80 days. The design of the low background thermal neutron detection system is introduced below.

Received 20 November 2016, Revised 29 December 2016
* Supported by National Natural Science Foundation of China (11475094)
1) E-mail: cengzm07@163.com
2) E-mail: gonghui@tsinghua.edu.cn
3) E-mail: leejm@mail.tsinghua.edu.cn
4) E-mail: yueq@mail.tsinghua.edu.cn
5) E-mail: zengzhi@tsinghua.edu.cn
6) E-mail: chengjp@mail.tsinghua.edu.cn

2 Design of the detection system

2.1 Low background thermal neutron detector

We used a ^{3}He proportional counter tube as the thermal neutron detector, for its large absorption cross section for thermal neutrons and low sensitivity to other types of radiation. Oxygen-free copper (OFC) was selected as the tube material, to reduce the background from the radioactivity of wall material, which constitutes the main background of the detector. Figure 1 shows the energy spectrum of the detector in the pulsed thermal neutron beam at the Tsinghua Compact Pulsed Hadron Source (CPHS). The neutron is converted into charged particles (tritium and proton) through the nuclear reaction n+^{3}He$\longrightarrow$ T+p ($Q = 0.764$ MeV). As the tritium or proton might hit the tube wall before depositing all its energy inside the working gas, there is a tail at the left-hand side of the full energy peak, as shown in Fig. 1, which is known as the wall effect. It is expected to reduce the wall effect and improve the energy resolution for low flux ambient thermal neutron detection.

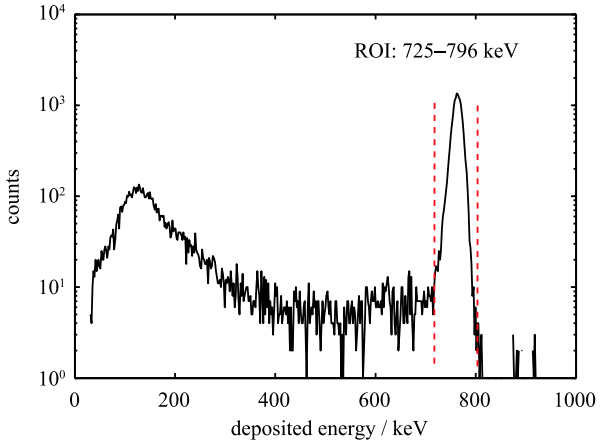

Fig. 1. (color online) Energy spectrum of the ^{3}He proportional counter tube in the thermal neutron beam. The peak in the ROI is the full energy peak and the left-hand peak is caused by γ.

The fraction of events that interact with the counter wall for a primary ionization track length R is approximately R/D, if D is the counter internal diameter assumed to be larger than R [9]. Adding a heavy noble gas into the working gas will significantly reduce the wall effect. A gas mixture of 5 atm Ar and 4 atm ^{3}He was employed as the working gas for low wall effect (11.5% given by GEANT4 [10] calculation), relatively low γ detection efficiency and working voltage.

The energy resolution of the ^{3}He proportional tube is influenced by many non-ideal factors and the uniformity and smoothness of the anode wire prove to be critical [9]. Gold-plated tungsten wire was selected as the anode wire and long field tubes were used at both ends of the detector to improve the energy resolution.

In order to decide the optimal working voltage for the detector, the pulse amplitude spectra under different working voltages were measured. The measurement results of FWHM resolution of the full energy peak and the gas multiplication factor are shown in Fig. 2 and Fig. 3 respectively. The best energy resolution performance is achieved at the smallest possible voltage to keep electronic noise to a negligible level. The space charge effect plays an important role in the deterioration of energy resolution with higher working voltages. To achieve the best energy resolution, 1650 V was selected as the optimal working voltage, under which the gas multiplication factor is about 7.

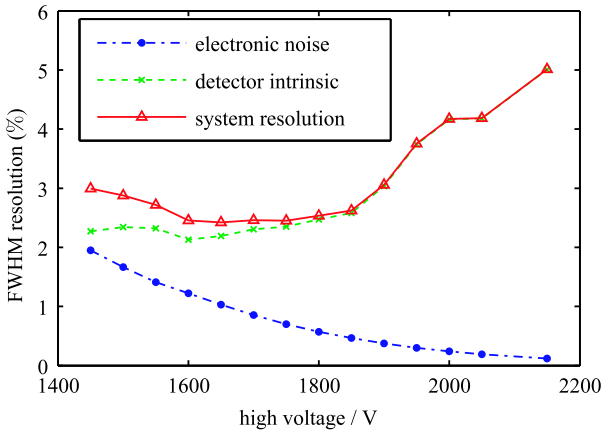

Fig. 2. (color online) FWHM resolution with working voltage. The solid line represents the measured FWHM resolution of the full energy peak, the dash-dotted line represents the electronic noise contribution, and the dotted line represents the calculated intrinsic resolution of the detector.

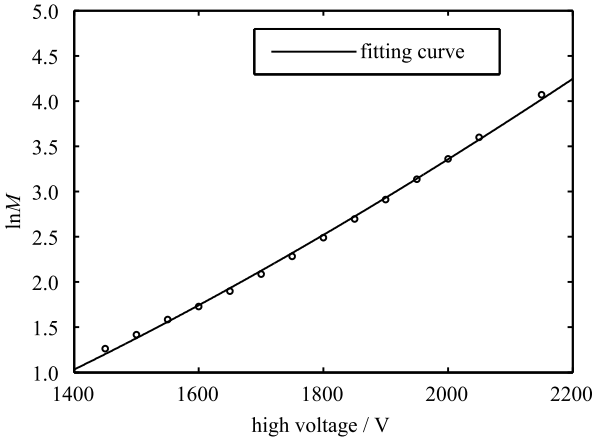

Fig. 3. Gas multiplication factor under different working voltages.

A ^{4}He proportional counter tube, which is identical to the ^{3}He proportional counter tube in all other aspects,

was made to analyse the background of the ^{3}He tube. The parameters of the designed low background thermal neutron detector are summarised in Table 1.

Table 1. Detector parameters.

	^{3}He tube	^{4}He tube
size	$\phi 25.4 \times 1121$	$\phi 25.4 \times 1121$
sensitive volume	$\phi 23.4 \times 1034$	$\phi 23.4 \times 1034$
filling gas	4 atm ^{3}He+5 atm Ar	4 atm ^{4}He+5 atm Ar
wall material	OFC	OFC
anode	ϕ25 μm gold-plated tungsten	ϕ25 μm gold-plated tungsten
woking voltage	1650 V	1650 V
FWHM resolution	2.4%	
wall effect	11.5%	

2.2 Readout electronics

A short high voltage cable with a length of 5 cm was utilised to connect the pre-amplifier with the detector for flexibility and low electronic noise consideration. The digitizer together with the high voltage module were encapsulated in a small cast aluminium box and connected to the laptop via an Ethernet cable. Two cables are needed for each pre-amplifier: one for high voltage and another for signal output and power supply. The output of the charge sensitive pre-amplifier is directly fed into the 80 MHz 14-bit digitizer without shaping circuit so as to get time and energy information simultaneously. Firmware on the FPGA monitors the digitalized waveform of each channel and samples a fixed length before and after the point where the waveform value crosses the preset threshold. The sampled waveform data is transferred to the laptop via Gigabit Ethernet based on SiTCP [11]. QT-based DAQ software on the PC has been developed which can support multiple digitizers simultaneously. Figure 4 shows the block diagram of the readout electronics system.

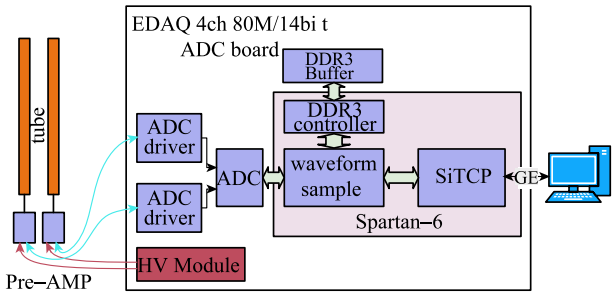

Fig. 4. (color online) Block diagram of the readout electronics system.

The readout electronics system was designed for long-term stable operation and easy maintenance in the underground laboratory under construction. A UPS device is used as the system power supply, and the system can recover from a power outage accident automatically. The data files on the disk are continuously checked by a monitor program and a system restart will occur if any abnormal situation happens. A warning lamp indicates whether the system needs manual intervention and all the details are logged for diagnosis.

2.3 Sensitivity calibration

The sensitivity of the detector to ambient thermal neutron field should be determined to calculate the thermal neutron flux from the measured result. A Monte-Carlo program was developed based on the GEANT4 toolkit [10] and a fully thermalized uniform isotropic neutron field was accepted as an approximation for the ambient thermal neutron field in a deep underground cave. The sensitivity was found to be 106 cm^2 and the details were described in Ref. [7].

In the measurement of low flux ambient thermal neutron field, neutrons were counted in the ROI around the full energy peak to reduce the background counting rate. The ratio of the number of neutrons registered in the ROI to the total number of neutrons captured by the detector, called ROI efficiency, can be determined by the results for the thermal neutron source. Figure 5 shows a scatter plot of the pulse risetime and the deposited energy, obtained from the same data source as Fig. 1. As the track length of electrons in the working gas is much longer than that of protons and tritium with the same energy, the risetime of γ events is larger than that of thermal neutrons, which can be used to discriminate thermal neutron events from γ events [12]. Points below the solid red line were counted as thermal neutron events, and the error proves to be less than 0.5% due to

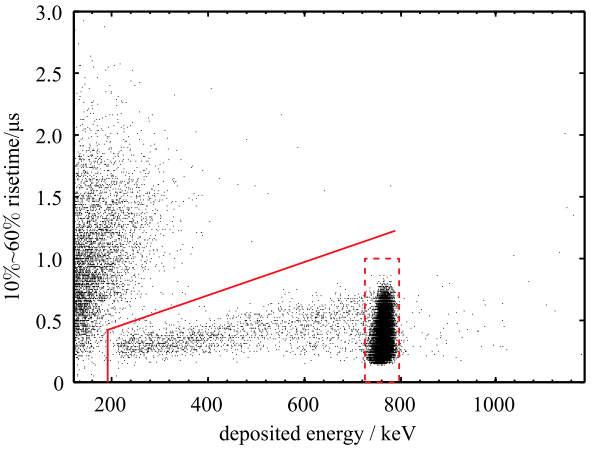

Fig. 5. (color online) Scatter plot of the pulse risetime and the deposited energy obtained from the same data as Fig. 1. γ events lie in the left-hand triangle, and points under the solid red line are neutron events. ROI efficiency can be calculated from this scatter plot.

the selection of the separating line between γ and neutron events. Points in the red dashed frame were counted as ROI neutron events. The ROI efficiency was conservatively determined to be $(87.93 \pm 1.94)\%$, considering possible distortion of the energy spectrum obtained during long-term measurements.

3 Experimental setup and results

The rock excavation work of CJPL-II was completed in July 2016. Four large experimental halls, each 14 m $\times$ 14 m $\times$ 130 m, have been built and the rock bolting work has just been finished. The low background thermal neutron detection system was installed in Lab Hall No. 3 before the installation of a waterproof plate and steel support structure. A sketch map of CJPL-II and the experiment site is shown in Fig. 6. The system accumulated data from July 27, 2016 to October 23, 2016 and the effective measurement time was about 80 days.

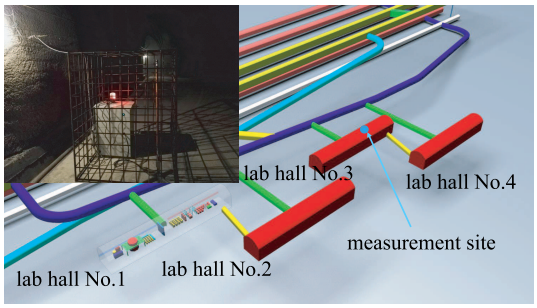

Fig. 6. (color online) Thermal neutron detection system installed in Lab Hall No. 3 (top left), and a sketch map of CJPL-II. The four Lab Halls and the main traffic tunnel are connected through auxiliary tunnels.

The measured energy spectra are shown in Fig. 7, and the spectra of the ^{3}He and ^{4}He proportional counters are very similar, with a correlation coefficient of 0.958. The average ROI count rate of the ^{3}He proportional counter tube is 80±1 cpd. The α background in the ROI has been extrapolated to be 1.69 ± 0.03 cpd from the background counts in the region between 1.0 MeV and 3.2 MeV. This extrapolation method can be verified by the results from the energy spectrum of the ^{4}He proportional counter tube. The α background in the ROI for the ^{4}He tube is extrapolated to be 1.43 ± 0.02 cpd from the background counts in the region between 1.0 MeV and 3.2 MeV. The actual ROI count rate of the ^{4}He tube is 1.45±0.13 cpd, in agreement with the extrapolated value. Different inner surface pollution situations during the manufacturing process might be one of the reasons causing the different background levels between the ^{3}He and ^{4}He tubes. Taking into account the ROI efficiency and the sensitivity, the ambient thermal neutron flux at the measurement site in Lab Hall No. 3 of CJPL-II after rock bolting is $9.76 \pm 0.12(\text{statistical}) \pm 0.22(\text{systematic}) \times 10^{-6}\text{cm}^{-2}\cdot\text{s}^{-1}$, assuming the thermal neutron field is fully thermalized, uniform and isotropic.

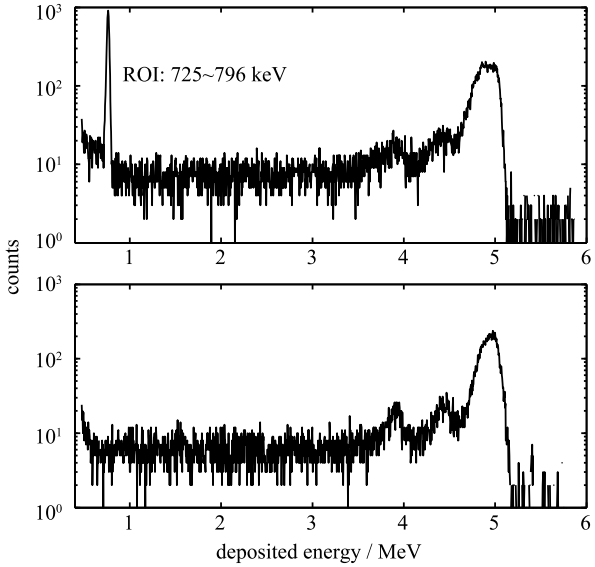

Fig. 7. Energy spectra obtained from measurements at CJPL-II. The upper part is the result from the ^{3}He tube and the bottom part the result from the ^{4}He tube. The FWHM resolution of the thermal neutron peak in the ROI is 3.4%. The flat region from 1 MeV to 3.2 MeV was selected for the extrapolation method.

The sensitivity of the detector is relatively high with low background rate, which makes it possible to observe the variation of thermal neutron flux. Figure 8 examines the ROI count of the ^{3}He tube day by day. The P-value of chi squared test against the hypothesis that the neutron flux is constant with time is 0.12, not significant enough to reject the constant assumption.

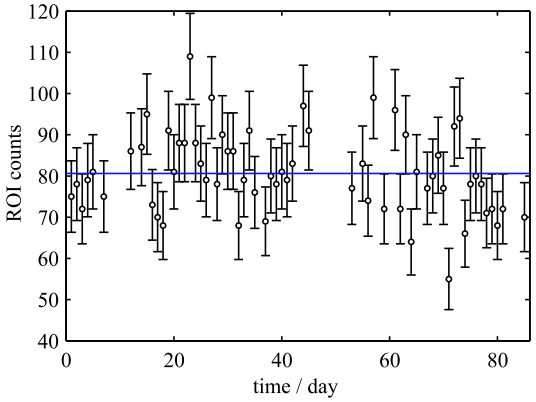

Fig. 8. (color online) ROI count of the ^{3}He tube day by day. The solid blue line represents the average ROI count per day.

4 Conclusion

The designed low background thermal neutron detection system is qualified to measure the low flux ambient thermal neutron field at CJPL-II in a relatively tough environment. The ambient thermal neutron flux measured at Lab Hall No. 3 of CJPL-II is $9.76\pm0.12(\text{statistical})\pm0.22(\text{systematic})\times10^{-6}\,\text{cm}^{-2}\cdot\text{s}^{-1}$, under the assumption that the neutron field is fully thermalized, uniform and isotropic. Nuclide activation caused by ambient thermal neutrons is an important background source for the planned tonne-scale high-purity germanium (HPGe) dark matter direct search experiment. A massive liquid nitrogen passive shield is therefore planned to be built to protect the HPGe crystals from the environmental radiation. The ambient thermal neutron flux measured in this paper will be important for the design of the liquid nitrogen shield and the interpretation of the background of the dark matter search experiment.

References

1 H. S. Chen, Eur. Phys. J. Plus, **127**: 105 (2012)
2 Q. Yue, W. Zhao, K. J. Kang et al, Phys. Rev. D, **90**: 091701(R) (2014)
3 J. L. Liu, P. W. Xie, X. D. Ji et al, Physical Review Letters, **117**: 121303 (2016)
4 J. M. Li, X. D. Ji, W. Haxton et al, Physics Procedia, **61**: 576–585 (2015)
5 S. R. Hashemi-Nezhad, L. S. Peak, Nuclear Instruments and Methods in Physics Research A, **357**: 524–534 (1995)
6 R. Lemrani, M. Robinson, V. A. Kudryavtsev et al, Nuclear Instruments and Methods in Physics Research A, **560**: 454–459 (2006)
7 Z. M. Zeng, H. Gong, Q. Yue et al, Nuclear Instruments and Methods in Physics Research A, **804**: 108–112 (2015)
8 A. Best, M. Junker, K. Kratz et al, Nuclear Instruments and Methods in Physics Research A, **812**: 1–6 (2016)
9 D. Mazed, S. Mameri, R. Ciolini, Radiation Measurements, **47**: 577–587 (2012)
10 S. Agostinelli, J. Allison, K. Amako et al, Nuclear Instruments and Methods in Physics Research A, **506**: 250–303 (2003)
11 T. Uchida and M. Tanaka, Development of TCP/IP processing hardware, 2006 IEEE Nuclear Science Symposium Conference Record, San Diego, CA, 2006, p. 1411–1414.
12 T. J. Langford, C. D. Bass, E. J. Beise et al, Nuclear Instruments and Methods in Physics Research A, **717**: 51–57 (2013)